Vol. 56: 91–101, 2013
doi: 10.3354/cr01144

CLIMATE RESEARCH
Clim Res

Published online March 12

# Tree-ring based summer minimum temperature reconstruction for the southern edge of the Qinghai-Tibetan Plateau, China

**Li-Xin Lv, Qi-Bin Zhang***

**State Key Laboratory of Vegetation and Environmental Change, Institute of Botany, Chinese Academy of Sciences, Beijing 100093, China**

ABSTRACT: Information about historical summer temperature variability is rare on the Qinghai-Tibetan Plateau (QTP). Here we report a 290 yr summer (June to August) mean minimum temperature (SMMT) record reconstructed from tree-ring widths of alpine juniper *Sabina squamata* in Yadong County at the southern edge of QTP, China. The reconstruction accounts for 51.2% of the SMMT variance in the instrumental period from 1956 to 2002. Five cold intervals in 1725–1734, 1745–1789, 1817–1825, 1860–1869 and 1967–1978, and 4 warm intervals in 1735–1744, 1790–1816, 1870–1879 and 1990–2002 were identified. Wavelet analysis of the reconstructed temperatures suggested the existence of 2 to 7 yr cycles in discontinuous periods and 20 to 25 yr cycles in the 1850s to 1880s. The reconstructed summer temperature variations were consistent with other temperature records from tree rings, ice cores and glacier activities on the QTP, which demonstrate the fidelity of the reconstruction and suggested that the climate in the study region was part of a large-scale climate system. The 1980s to 2000s were the warmest period in the last 3 centuries in our tree-ring records, but the amplitude of the warming was still within the natural variation.

KEY WORDS: Global warming · Qinghai-Tibetan Plateau · Climate reconstruction · Minimum temperature · Summer temperature · *Sabina squamata* · Tree rings · Yadong County



## 1. INTRODUCTION

The Qinghai-Tibetan Plateau (QTP), with an average elevation of >4000 m a.s.l. and an area of ~2.5 × $10^6$ $km^2$, is the highest and most extensive highland in the world and exerts an imposing influence on regional and global climate through thermal and mechanical forcing mechanisms (Yeh & Gao 1979, Yanai & Li 1994, Wu & Zhang 1998, Feng & Hu 2005, Xu et al. 2010). Information about the QTP climate helps establish the link between plateau climate and larger spatial scale climate systems like the Indian Summer Monsoon (ISM) and the El Niño–Southern Oscillation (ENSO). However, the instrumental climate records on the QTP are sparse and in most cases limited to the past 50 yr. Moreover, the majority of the instrumental records originate from the eastern rim of the QTP, and only a few instrumental data are available from other parts. Therefore, long-term high-resolution climate proxy data are needed to increase the spatiotemporal coverage of the pre-instrumental climate history on the QTP.

Tree rings and ice cores are the 2 main high resolution climate proxies on the QTP. Compared to ice cores, tree rings are characterized by the spatially wide distribution of trees and by their annual resolution and precise dating, from which long palaeoclimatic records can be developed (Zhang et al. 2003, Sheppard et al. 2004, Shao et al. 2007, Liu et al. 2009), as tree rings contain temperature signals on the QTP (Gou et al. 2008, Liu et al. 2009, Li et al. 2011). Comparison of long-term climate histories

*Corresponding author: Email: qbzhang@ibcas.ac.cn

over different parts of the QTP helps understanding the varying influence area of climatic circulation including ISM, ENSO, and the mid-latitude westerlies (Holmes et al. 2009).

On the southeast QTP, Helle et al. (2002) found that a short warm phase between 1200 and 1300 corresponded to the 'Mediaeval Warm Period' and a larger cool phase from AD ~1450 to 1600 corresponded to the 'Little Ice Age' with a short recurring episode ~1850. Bräuning & Mantwill (2004) reconstructed the late summer (August and September) temperature and rainfall from a network of 22 maximum latewood density (MLD) chronologies of high-elevation conifer sites. They found that the increase of ISM activity after 1980 was unprecedented during the past 350 yr. A reconstruction of the mean summer (June to August) temperature from Georgei fir *Abies georgei* var. *smithii* tree-ring width chronology at the timberline in the Sygera Mountains showed that the last decade was the warmest period in the past 242 yr (Liang et al. 2009).

On the northeast QTP, Liang et al. (2008) reconstructed the mean summer minimum temperature for the past 379 yr based on tree-ring data in the source region of the Yangtze River, and found that the coldest period was the interval of 1816 to 1822, which might be related to the influence of the Tambora eruption in Indonesia in 1815.

On the central QTP, Yang et al. (2009) combined the data of an ice core from the Puruogangri ice field and regional tree rings and found that the period 1725–1775 was one of the most prolonged cool periods during the past 400 yr and corresponded to maximum 'Little Ice Age' glacier advance of monsoonal temperate glaciers of the QTP.

On the western QTP, Yang et al. (2010) reconstructed a 622 yr mean January–June temperature history and found that solar and volcanic activity played an important role in modulating regional temperature variation. In the western Himalayas, spring (March to May) temperature reconstructions from tree rings of Himalayan cedar *Cedrus deodara*, however, indicated a decreasing trend in temperature variations since the 1960s (Yadav & Singh 2002, Yadav et al. 2004).

The climate on the QTP is controlled by many drivers and the spatial pattern is complicated; even opposite trends in temperatures were witnessed in different parts (e.g. abnormal warming on the SE QTP and cooling trends in the western Himalayas since the 1960s). The southern rim of the QTP is strongly exposed to the ISM; longer climate data in this region would contribute to a better understanding of the atmospheric circulation behavior in lower frequencies. Most tree-ring studies on the QTP are confined to the eastern part to date, and climate reconstruction in the southern edge is scarce.

Here, we report a summer temperature reconstruction based on alpine juniper *Sabina squamata* in Yadong County, southern edge of the QTP (Fig. 1).

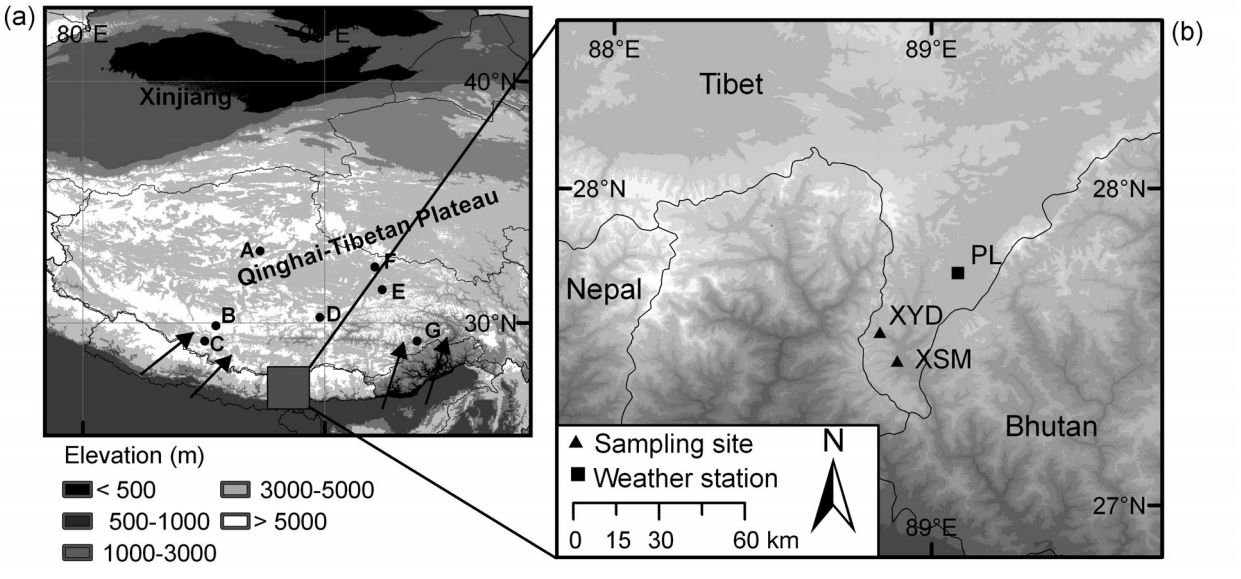


Fig. 1. Study area. (a) Arrows: direction of Indian Summer Monsoon (ISM); A: ice core recovered from Puruogangri ice field; B: Dasuopu ice core; C: Nepal temperature reconstruction (Cook et al. 2003); D: summer temperature reconstruction in Sygera Mts (Liang et al. 2009); E: Aug–Sep temperature reconstruction in Changdu Prefecture (Wang et al. 2010); summer temperature reconstructions in F: the source region of the Yangtze River on the Tibetan Plateau (Liang et al. 2008), and G: the central Hengduan Mountains (Fan et al. 2009). (b) Pali weather station (PL; 27°44′N, 89°05′E; 4300 m a.s.l) and tree core sites (XSM and XYD)

Summer temperature in this region is highly affected by the strength of the ISM (Feng & Hu 2005, Holmes et al. 2008). To our knowledge, this reconstruction is the first summer temperature proxy record at the southern edge of the QTP. It will contribute to the accumulation of proxy climate records for the southern QTP and benefit our understanding of the regional climate variations and their relationships with larger scale climate circulations in an extended temporal background.

## 2. MATERIALS AND METHODS

### 2.1. Study area and tree-ring sampling

Instrumental record from Pali weather station for the period 1956–2008 shows that monthly mean air temperature ranges from −8.6°C in January to 8.0°C in July, and annual mean air temperature is 0.9°C. Mean annual precipitation is 423 mm, with ~72% of the precipitation falling during the monsoon season (June to September) (Fig. 2). Unequal trends in the summer maximum and minimum temperature were observed at 4 Stations during the last several decades (Fig. 3). Increase in mean minimum temperature was prominent at all the stations, suggesting a similar summer warming trend in this region.

Field survey was carried out in the summer of 2003. Increment core samples were collected from alpine juniper *Sabina squamata* at 2 sites (27.45–27.55°N, 88.84–88.89°E) 15 km apart in Yadong County (Fig. 1). Alpine juniper is a cold- and drought-tolerant conifer on southern aspects of mountains, with a canopy height of ~10 to 15 m and canopy coverage of ~20 to 30%. In order to obtain long tree-ring series, cores were extracted from trees with large stem diameter and growing at locations of shallow layered soil and high altitude of the forest distribution. One core per tree and a total of 42 trees were cored from the 2 sampling sites (22 trees from site XSM, 20

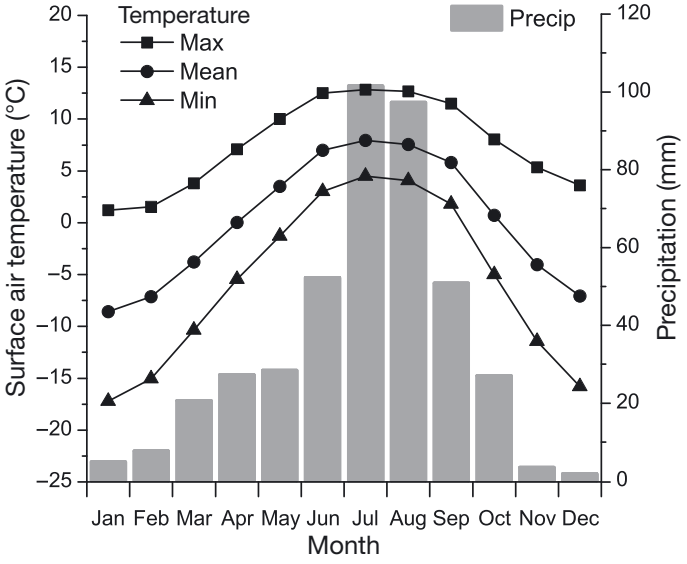


Fig. 2. Climatic diagram of Pali weather station (4300 m a.s.l.) in Yadong County, southern Tibet, southwestern China 1956–2008. Mean annual temperature (MAT): 0.9°C; mean annual precipitation (MAP): 423 mm

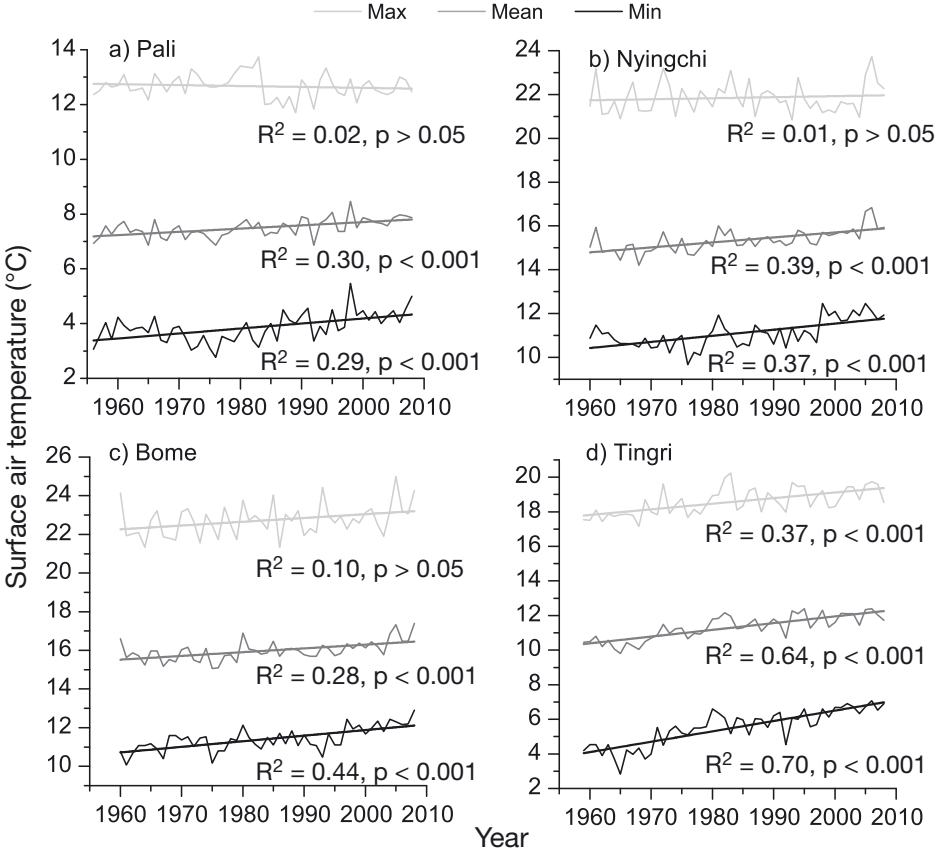


Fig. 3. Linear trends of summer temperature variation (Jun–Aug) recorded at (a) Pali (27° 44′ N, 89° 05′ E; 4300 m a.s.l.), (b) Nyingchi (29° 40′ N, 94° 20′ E; 2991 m a.s.l.), (c) Bome (29° 52′ N, 95° 46′ E; 2736 m a.s.l.), and (d) Tingri (28° 38′ N, 87° 05′ E; 4300 m a.s.l.) in southern Tibet

trees from site XYD) with elevations ranging from ~3500 to 3650 m. There was little human interference with the forest in this restricted region because of the vicinity to the national border.

### 2.2. Development of tree-ring chronology

In the laboratory, the cores were air-dried, mounted on wooden slots, and polished by progressively finer sandpaper till ring boundaries clearly showed up. With the aid of a microscope, the tree rings were crossdated by comparing the ring patterns among samples. The ring widths of each cross-dated sample were then measured to the nearest 0.001 mm by using a TA Unislide Measurement System (Velmex) and then quality checked by the COFECHA program, which calculates correlation coefficients between individual tree-ring series to present clues for potential errors in crossdating (Holmes 1983). The cores that could not be crossdated due to poor quality (e.g. having too many broken pieces, rotten wood) were excluded from further analysis.

Since the crossdated tree-ring samples from the 2 sites share similarities both within and between sites, and have a reasonable mean inter-serial correlation (R = 0.41), these tree-ring sequences were processed into 2 site chronologies and 1 composite tree-ring chronology separately by using the ARSTAN software (Cook 1985). The similarity between the 2 sampling sites is illustrated by 50 yr moving correlations (Fig. 4a–c). In order to remove age-related growth trends, while preserving most variations that are likely related to climate, a flexible cubic smoothing spline with 50% frequency-response cut-off at ⅔ of the serial length was used (see Cook & Kairiukstis 1990, p. 110–118). Tree-ring indices of each sample were obtained by calculating divisions between the ring-width measurements and the fitted splines. All detrended series were then averaged to obtain a standard chronology by computing the biweight robust mean in order to reduce the influence of outliers (see Cook & Kairiukstis 1990, p. 123–127). Variance stabilization (Osborn et al. 1997) was applied to adjust for changes in variance associated with declining sample size (number of trees) over time.

Descriptive statistics were calculated to assess the quality of the standardized chronology (see Cook & Kairiukstis 1990, p. 137–153). Mean sensitivity (MS) is an indicator of the relative change in ring widths between consecutive years, and a higher MS suggests more sensitivity of tree ring growth to interannual environmental changes. The first-order autocorrelation (AC1) assesses relationship between growth in one year and its previous year. Common signal strength was evaluated by mean inter-series correlation ($R_{bar}$) and by the percent variance explained by the first principal component (PC1). The expressed population signal (EPS) and signal-to-noise ratio (SNR) are functions of R and sample size, and evaluate the signal strength of the chronology. PC1 and SNR were calculated for the common period 1851–2000. The median segment length (MSL) is a useful diagnostic for determining the maximum low-frequency signal resolvable in a tree-ring chronology (Cook et al. 1995). The subsample signal strength statistic (SSS) >0.85 (equivalent to allowing a maximum additional reconstruction

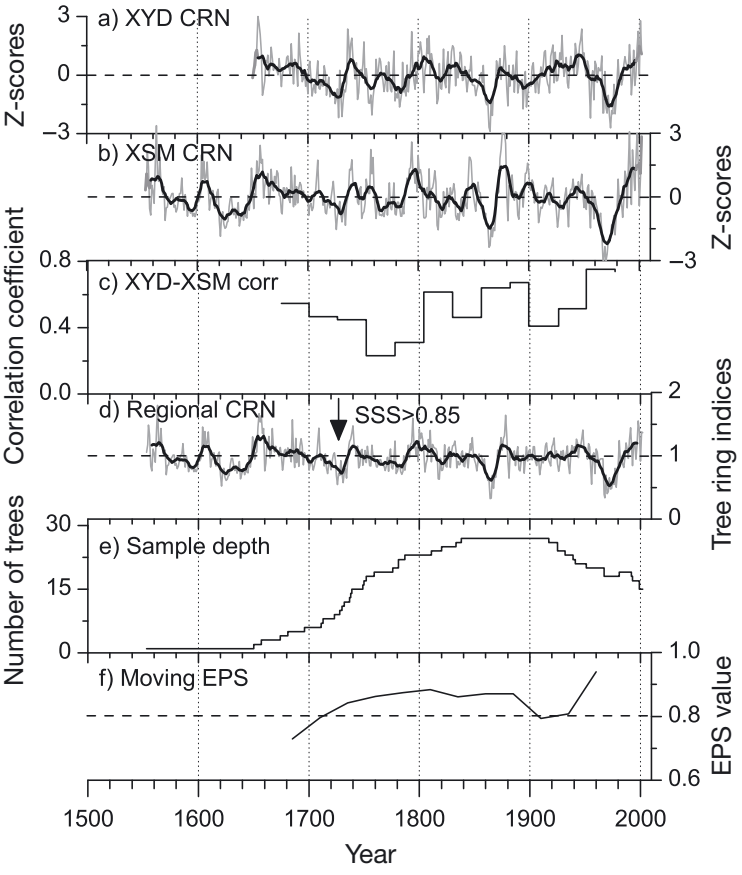


Fig. 4. (a,b) XYD and XSM site chronologies, (c) 50 yr moving correlations between site chronologies (CRN), (d) regional CRN for Yadong, and (e) sample depth and (f) running expressed population signal (EPS) of the regional CRN. Bold line: 11 yr moving average. Arrow: point after which Subsample Signal Strength (SSS) > 0.85, equal to a minimum of 8 trees. EPS value was calculated using a 50 yr sliding window with 25 yr lag. Reference line at 0.8 in the EPS means that tree-ring samples used in chronology building represent 80% of the population signal

uncertainty of 15%) was employed to assess the signal strength loss caused by reduced replication at more remote time periods, and to determine the reliable period of the chronology (Wigley et al. 1984, see Cook & Kairiukstis 1990, p. 151).

### 2.3. Climate–growth relationship

The relationships between tree-ring indices and climate variables were analyzed using correlation analysis for the period 1956–2002. The climate variables include monthly mean, mean maximum and mean minimum temperature, and monthly total precipitation from Pali weather station (Fig. 2). The climate data from previous October to current September were used for the analysis, as the climate conditions of the previous year may have effects on tree-ring growth of the current year (Fritts 1976). Bootstrapping was used to test the significance of the response coefficients by examining the distribution of the coefficients calculated from a large number of subsamples randomly selected with replacement from the initial data set (1000 replications in this study) (Efron 1979). This method has advantages when the statistical properties of the data are not well understood. The calculation and significance testing was done using DendroClim2002 (Biondi & Waikul 2004).

Spatial extent of the climate–growth relationship was examined by calculating the correlation fields between tree-ring indices and spatially gridded climate data for the common period 1956–2002 using the KNMI climate explorer (http://climexp.knmi.nl). The gridded climate data were obtained from the CRU TS 3 dataset (Mitchell & Jones 2005), which covers the period of 1901 to 2006; however, most of the instrumental records do not predate the 1950s. The CRU data are thus most reliable in this region since the 1950s.

### 2.4. Establishment of transfer function

The climate variable that has the highest correlation with the tree-ring chronology was selected for climate reconstruction. A linear regression was used to develop the transfer function in which the tree-ring chronology was the independent variable and the climate for reconstruction was the dependent variable. The climate and tree-ring data used for developing the transfer function were from 1956–2002. In consideration of shortness of the instrumental record, verification statistics were calculated over multiple leave-one-out regressions (Michaelsen 1987) as follows: Pearson's correlation (r), variance explained ($R^2$), adjusted variance explained ($R^2_{adj}$), root mean square error (RMSE), reduction of error (RE), sign test (SN) and product means test (PMT) (see Cook & Kairiukstis 1990, p. 178–185).

### 2.5. Analysis of the reconstructed climate

Past climate was reconstructed by applying the tree-ring chronology into the transfer function. We assume that the growth–climate relationship is consistent through time, both when the trees are young and old (Esper et al. 2008, Yu et al. 2008). To characterize the patterns of variation in the reconstructed climate, regime shift analysis was conducted using the Shift Detection Program version 3.2 (www.beringclimate.noaa.gov/regimes/). The algorithm for the program is based on sequential Student's *t*-tests that can signal a possibility of a regime shift in mean values through time (Rodionov 2004). The sliding window for calculating the *t*-tests was 10 yr, and the significance level was $p < 0.05$. The climate states and abrupt changes were compared with the pattern of climate change reported in other studies around the region.

Wavelet analysis was performed to identify the temporal characteristics of frequency signals in the reconstructed summer mean minimum temperatures (SMMTs) (Torrence & Compo 1998). The wavelet function used in the study is a Morlet wavelet with a wave number of 6, and the significance was tested at the 95% confidence level against a red-noise background. The wavelet analysis was processed by the online program at http://paos.colorado.edu/research/wavelets/.

## 3. RESULTS

### 3.1. Tree-ring width chronology

A total of 27 increment cores from the 2 sampling sites were successfully crossdated. The other 15 cores had too many broken pieces, rotten sections and irregular growth specific to individual trees. Based on these 27 cores, a 450 yr (1553–2002) standard chronology was developed (Fig. 4). The mean sensitivity of tree-ring series is 0.232, indicating that the tree tings are responding to environmental changes. The values of $R_{bar}$ (0.326) and PC1 (35.3%) indicate that the tree rings contain useful information

about common environmental change. The number of samples was lower back in time, due to age of the trees, and the chronology was truncated to exclude the years that have <8 sample replications (SSS > 0.85). The resultant chronology was 290 yr in length (1713–2002) and the 50 yr moving EPS was >0.8 in most years (Fig. 4). The MSL is 246 yr, indicating that multi-decadal to century scale low frequency signals are preserved in the chronology.

### 3.2. Relationship between tree-ring growth and climate

Results of the correlation analysis and significance test by the bootstrap method showed that tree-ring growth was most significantly correlated with SMMT ($r = 0.72$, $p < 0.05$) (Fig. 5c). No significant correlations were found between tree-ring growth and monthly mean maximum temperature (Fig. 5a). In terms of precipitation, tree-ring growth was only weakly correlated with January precipitation ($r = 0.22$, $p < 0.05$) (Fig. 5d).

The standardized tree-ring chronology and instrumental SMMT showed good agreement in the common period 1956–2002 ($R^2 = 0.52$, $p < 0.01$). Residuals of 10 yr low pass filters from both tree-ring chronology and instrumental data also indicated significant climate signals preserved in the tree rings at inter-annual scale ($R^2 = 0.27$, $p < 0.01$) (Fig. 6).

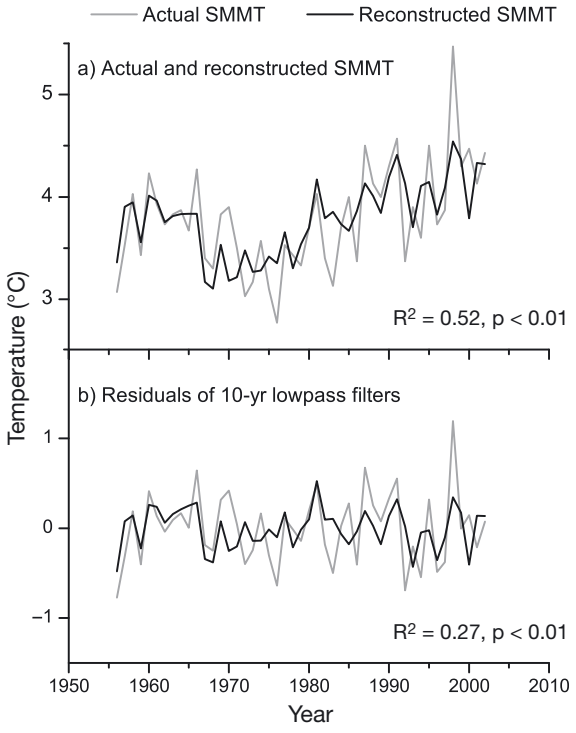


Fig. 6. Actual and reconstructed summer mean minimum temperature (SMMT) for 1956–2002

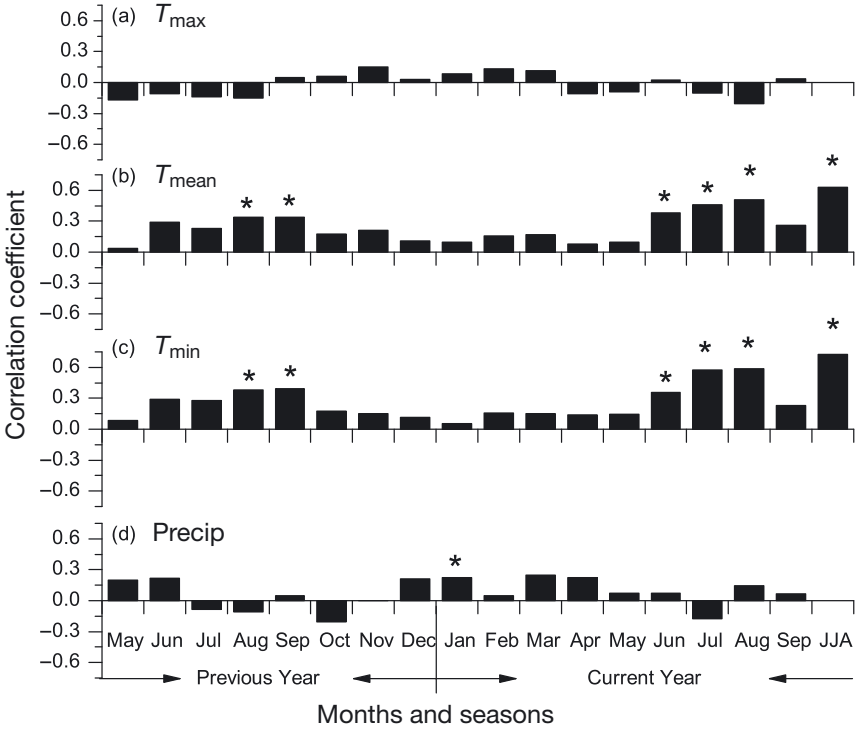


Fig. 5. Correlations between tree-ring width indices and monthly (a) maximum ($T_{max}$), (b) mean ($T_{mean}$) and (c) minimum ($T_{min}$) temperatures, and (d) precipitation. Meteorological data were derived from Pali Stn. Note: JJA: Jun–Aug. *$p < 0.05$ tested by bootstrap method

Spatial correlation field of tree-ring indices with regionally gridded monthly mean minimum temperature for the period 1956–2002 showed that the tree rings were correlated with SMMT in the study region (Fig. 7). These results further indicated that the Yadong tree-ring chronology represented SMMT variation for a large territory on the QTP.

### 3.3. Reconstruction of summer minimum temperature

Transfer function was developed using Yadong tree-ring chronology and SMMT data for 1956–2002. In the leave-one-out cross validation, the values of r, $R^2$ and $R^2_{adj}$ are close to the values found in the calibration model. Sign test and

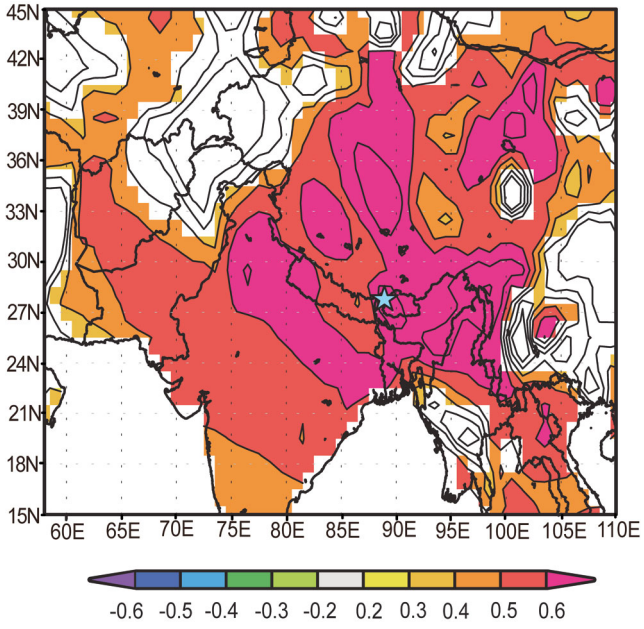


Fig. 7. Spatial correlations of reconstructed summer (June–Aug.) mean minimum temperatures (SMMTs) with regional gridded SMMTs from the CRU TS 3 dataset (Mitchell & Jones 2005) for 1956–2002. Insignificant correlations ($p < 0.05$) were masked out. Analyses were performed using the KNMI climate explorer. Blue star: study area

product mean test are significant at $p < 0.01$. RMSE is 0.371 and RE is 0.456 (Table 1). All these verification statistics indicated that the calibration regression model was stable and reliable (see Cook & Kairiukstis 1990, p. 178–185). Therefore using the data from the whole period 1956–2002, the transfer function was developed as follows:

$$SMMT = 1.181TR + 2.708 \quad (1)$$

where TR is the tree-ring chronology. Applying the tree-ring data into the transfer function, the SMMT was reconstructed for the period 1713–2002 (Fig. 8b). The reconstructed SMMT explained 51.2% (50.1% after adjusted for loss of degrees of freedom) of the variance in the observed temperature data (Table 1).

Table 1. Calibration and verification statistics of summer mean minimum temperature (SMMT) reconstruction model using the leave-one-out method during the period 1956–2002. r = Pearson's correlation, $R^2_{adj}$ = adjusted variance explained, DW: Durbin–Watson test, RE: reduction of error, ST: prediction sign test, '+': pair of actual and predicted temperatures showed same sign of departures from their respective mean values; '–': different sign of departures; PMT: *t*-value of product means test. $^{**}p < 0.01$

| | r | $R^2$ | $R_{adj}^2$ | DW | RMSE | RE | ST | PMT |
|---|---|---|---|---|---|---|---|---|
| Calibration | 0.716** | 0.512 | 0.501 | 2.102 | – | – | – | – |
| Verification | 0.676** | 0.457 | 0.445 | – | 0.371 | 0.456 | 34+/13–** | 3.9** |

### 3.4. Variation in the summer minimum temperature

Regime shift analysis of the CRU data showed that abrupt shifts from high to low temperatures occurred in 1963–1964, and shifts from low to high temperatures occurred in 1918–1919, 1978–1979, 1997–1998 (Fig. 8a). Regime shift analysis of the reconstructed SMMT showed that abrupt shifts from high to low temperatures occurred in 1724–1725, 1744–1745, 1816–1817, 1859–1860, 1879–1880 and 1966–1967, and shifts from low to high temperatures occurred in 1734–1735, 1789–1790, 1825–1826, 1869–1870, 1978–1979 and 1989–1990 (Fig. 8b). These shifting points gave an objective criterion for detecting the warm/cold periods from the reconstructed temperature history. Two conspicuous cold periods, 1901–1918 and 1964–1978, were recognized in the CRU data (Fig. 8a). The reconstructed SMMT history suggests 4 periods with warm summers occurred in 1735–1744, 1790–1816, 1870–1879 and 1990–2002, and 5 periods with prolonged cold summers occurred in 1725–1734, 1745–1789, 1817–1825, 1860–1869 and 1967–1978 (Fig. 8b).

### 3.5. Wavelet transform of the reconstructed summer minimum temperatures

Wavelet analysis of the reconstructed SMMTs over 1713–2002 demonstrated the presence of pronounced inter-annual and multi-decadal periodicities in southern Tibet (Fig. 8c–d).

In some periods (during the 1780s, 1820s, 1880s, 1950s–1970s, 1985–2002), the signal of a ~4 yr cycle (~2–7 yr; Fig. 8c) is stronger than the others, while in the 1790s to 1810s, periodicities of ~8 yr (Fig. 8c) also have a stronger signal. In the 1850s to 1880s, significant bi-decadal cycles dominated the low frequency signals (Fig. 8c). Besides, a multi-decadal scale periodicity (~35–65 yr) also existed since the mid 1910s; however, most of the period is in the cone of influence (COI), where edge effects become important.

## 4. DISCUSSION

### 4.1. Influence of temperature on tree-ring growth

The relationship between tree-ring growth and climate variables may reflect the fact that tree

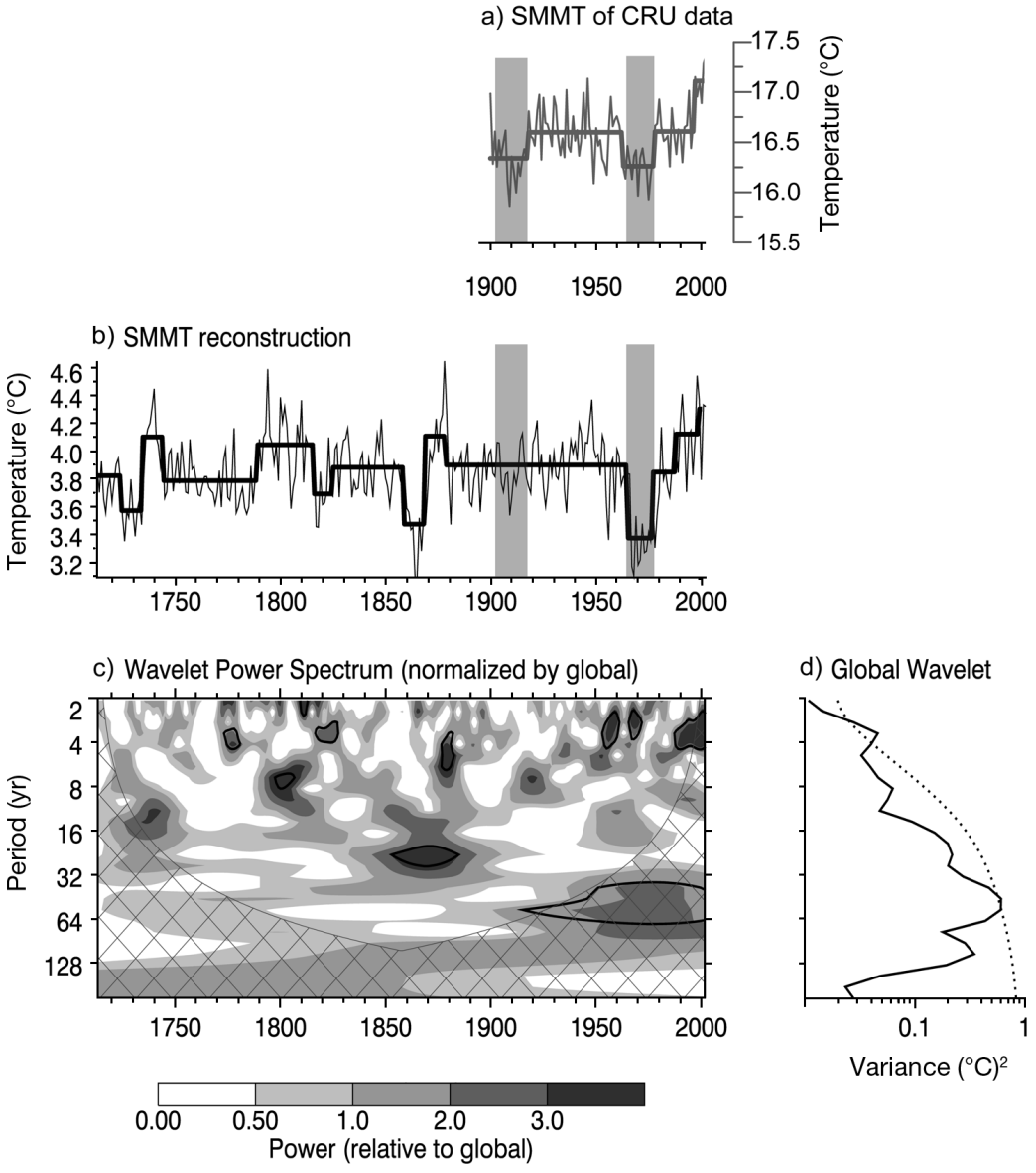


Fig. 8. (a) Raw values (curve) and regime shifts (bold stair line) of summer mean minimum temperatures (SMMTs) of CRU data for 1901–2006; (b) raw values and regime shifts, (c) wavelet power spectrum, and (d) global wavelet of the reconstructed SMMTs for 1713–2002 based on tree rings. Dotted line: significance for the global wavelet spectrum (solid line), assuming the same significance level and background spectrum as in (c). (a,b) Grey vertical bars: 2 cold periods based on the CRU data, which was extracted over an expanded study region (24–30° N, 80–100° E). (c) Cone-shaped net: areas of spectrum susceptible to effects of zero padding (Torrence & Compo 1998); black contours: 5% significance level, using a red-noise background spectrum

growth at the timberline is limited by the summer minimum temperature (Fig. 5c). A similar relationship between tree-ring growth and summer minimum temperature was reported for the QTP (Liang et al. 2008, 2010) and nearby region (Li et al. 2011). Low summer night air temperatures (minimum temperatures) result in low soil temperatures, which persist in daytime, especially in understory environments (Tranquillini 1979). In cold soils, leaf conductance is lower, leading to lower intercellular $CO_2$ concentrations and greater stomatal limitation of photosynthesis (DeLucia 1986, Day et al. 1989). Low summer soil temperature at the timberline can limit the growth of roots and their function in water uptake (Goldstein et al. 1985, Körner 1999, Körner & Paulsen 2004). At the timberline, minimum temperature is a critical factor affecting conifer tracheid division and enlargement by changing the timing and duration of the growing season (Deslauriers et al. 2003, Rossi et al. 2008).

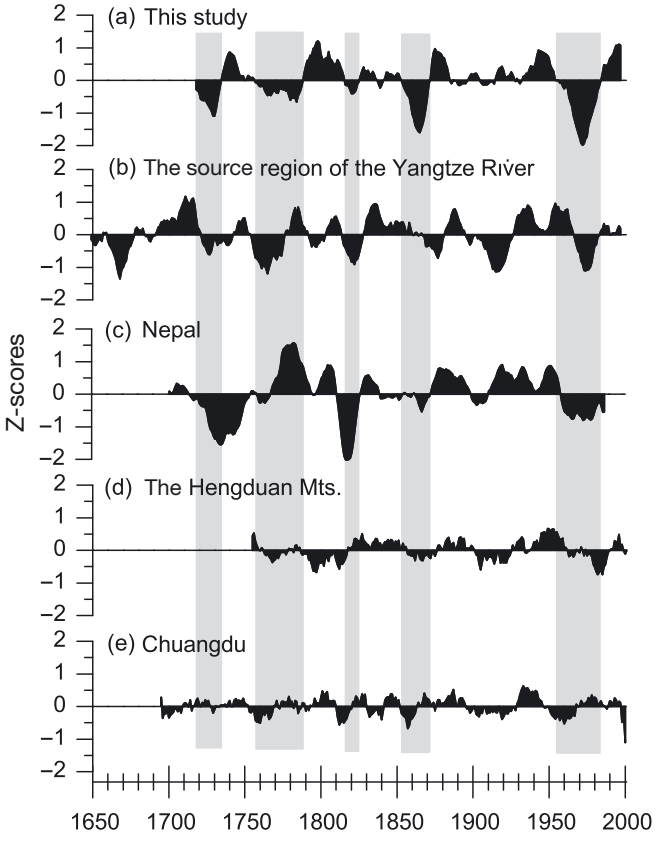


Fig. 9. Comparisons between summer mean minimum temperature (SMMT) reconstructions in (a) Yadong County with (b–e) other regional temperature records. All chronologies were smoothed by an 11 yr moving average (black areas). Grey bars: cold periods as indicated by the current reconstruction. Data sources: (b) Jun–Aug minimum temperature reconstruction in the source region of the Yangtze river (Liang et al. 2009); (c) Feb–Jun mean temperature reconstruction in Nepal (Cook et al. 2003); (d) Apr–Sep mean temperature reconstruction in Hengduan Mts. (Fan et al. 2009); (e) Aug–Sep mean temperature reconstruction in Changdu (Wang et al. 2010)

### 4.2. Comparison with other regional temperature records

Several tree-ring based temperature reconstructions have been reported on the QTP (Liang et al. 2008, Wang et al. 2010) and nearby regions (Cook et al. 2003, Fan et al. 2009). To compare decadal scale variations between these temperature reconstructions and the present study, each series was *Z*-scored and smoothed by 11 yr moving averages. Five conspicuous temperature minima were recognized in 1720s–1730s, 1750s–1780s, 1810s–1820s, 1860s and 1960s–1970s, according to the above criteria (Fig. 9a).

The most prominent cold summer in the 1960s to 1970s in the present study is consistent with low SMMTs in the source region of the Yangtze River, northeastern QTP (Liang et al. 2008) (Fig. 9b), and low pre-monsoon (February to June) temperatures in Nepal (Cook et al. 2003) (Fig. 9d). The second cold period in the 1850sto 1860s in our SMMT reconstruction corresponds to the low April–September temperatures in the Central Hengduan Mountains (Fan et al. 2009) (Fig. 9c). The cold phase in the 1850s to 1860s occurred in Nepal (Fig. 9c), Hengduan Mts. (Fig. 9d), and Changdu prefecture (Fig. 9e), but the duration and amplitudes were significantly lower than those in our study area.

A brief cold period that occurred during 1817–1825 in our reconstruction roughly corresponds to the most conspicuous minima in February–June temperatures in Nepal (Fig. 9d) (Cook et al. 2003), west of our study region (Fig. 1a). The cooling effect from the Tambora eruption was reported to account for this temperature drop (Cook et al. 2003, Liang et al. 2008).

The cold periods in the 1720s–1730s and 1750s–1780s in this study were also reported in the source region of the Yangze River, NE QTP, where the latter cold event was longer than in Nepal, but shorter than in Yadong (Fig. 9). The above 2 cold periods were also recorded by $\delta^{18}O$ on the central (Yang et al. 2009) and SW (Thompson et al. 2000) QTP.

Though the major cold periods in the SMMT reconstruction are corroborated by other paleoclimatic records, discrepancies exist in the timing and amplitude of temperature variations. The period 1900s–1910s was recorded as a cold one in the NE QTP (Liang et al. 2009), SE QTP (Fan et al. 2009, Wang et al. 2010) and Nepal (Cook et al. 2003), but not in our study area (Fig. 9).

Comparisons with tree-ring based temperature reconstructions over different regions suggest that the SMMT variations in the southern edge of the QTP resembled those of the southern and eastern QTP but differed from those in the western Himalayas (Yadav & Singh 2002), although this pattern was not stable through time due to local conditions.

### 4.3. Wavelet spectrum and possible climate drivers

Significant ($p < 0.05$) and unstable periodicities were detected both at interannual (2 to 7 yr) and multi-decadal scales (~20 yr) in the reconstructed SMMTs (Fig. 8c). This indicates a complex of driving forces controlling summer temperature variations in the study region. Among them, ISM has a close relationship with the summer temperatures in the

southern QTP (Feng & Hu 2005). The El Niño–Southern Oscillation (ENSO) is one of the most important factors contributing to interannual variation of the ISM (Lau & Nath 2000). The observed inter-annual periodicities in the reconstructed temperature variations fall within the range of the ENSO variability (Allan et al. 1996), suggesting a possible influence from ENSO systems. The ENSO-like signal was also detected in previous studies on the QTP (Zhang et al. 2000, Xu et al. 2010).

Due to a high radiation load at upper elevations and low latitudes, climate on the southern QTP is affected by solar activity. The periodicities ~20 yr in the 19th century and the coinciding regime shift in the late 1850s suggest that solar activity contributes to the formation of these cold events. The solar cycles were also previously recorded by tree rings on the QTP (Yang et al. 2010, Wang & Zhang 2011, Li et al. 2012).

## 5. CONCLUSIONS

Our study found that the annual growth rings of juniper trees in Yadong County were sensitive to SMMTs. The reconstructed 290 yr SMMT variation was compared with other temperature sensitive proxies on nearby regions. The comparisons suggest that summer warming since the 1960s is significant on both the southern and eastern QTP, but not in the western Himalayas. The period 1980s–2000s was likely the warmest period in the last 3 centuries, as seen in our tree-ring records, but the amplitude of the warming was still within the natural variations.

Possible climatic drivers of the summer temperatures at the southern edge of the QTP as detected in the wavelet analysis are ENSO systems (2 to 7 yr cycles), solar activities (7 to 11 yr cycles in the 1790s–1810s and 20 to 25 yr cycles in the 1850s–1880s). Besides, volcanic activities might also affect the summer temperature variation during the 1810s to 1820s in this region. The tree-ring data derived from this study contribute to the spatial coverage of climate proxies on the QTP, where the climate records are still sparse and short in length.

*Acknowledgements.* This research was supported by grants No. 30670365, 31170419 and 40631002 from the Natural Science Foundation of China. The climate data were obtained from the weather information center of China Meteorological Administration. We extend our thanks to Dr. E. Liang, Dr. L. Wang and Dr. Z.X. Fan for kindly providing data for comparison. We thank the whole field work team for hard work and great cooperation. We also thank the Tibetan Forestry Bureau for permitting field sampling.

LITERATURE CITED

Allan HL, Lindesay J, Parker D (1996) El Niño/Southern Oscillation and climate variability. CSIRO Publishing, Collingwood

Biondi F, Waikul K (2004) DENDROCLIM2002: a C++ program for statistical calibration of climate signals in tree-ring chronologies. Comput Geosci 30:303–311

Bräuning A, Mantwill B (2004) Summer temperature and summer monsoon history on the Tibetan plateau during the last 400 years recorded by tree rings. Geophys Res Lett 31:L24205, doi:10.1029/2004GL020793

Cook ER (1985) A time series analysis approach to tree-ring standardization. PhD thesis, University of Arizona, Tucson

Cook ER, Kairiukstis LA (1990) Methods of dendrochronology: applications in the environmental sciences. Kluwer Academic Press, Dordrecht

Cook ER, Briffa KR, Meko DM, Graybill DA, Funkhouser G (1995) The segment length curse in long tree-ring chronology development for paleoclimatic studies. Holocene 5:229–237

Cook ER, Krusic PJ, Jones PD (2003) Dendroclimatic signals in long tree-ring chronologies from the Himalayas of Nepal. Int J Climatol 23:707–732

Day TA, DeLucia EH, Smith WK (1989) Influence of cold soil and snowcover on photosynthesis and conductance in two Rocky Mountain conifers. Oecologia 80:546–552

DeLucia EH (1986) Effect of low root temperature on net photosynthesis, stomatal conductance and carbohydrate concentration in Engelmann spruce (*Picea engelmannii Parry*) seedlings. Tree Physiol 2:143–154

Deslauriers A, Morin H, Begin Y (2003) Cellular phenology of annual ring formation of *Abies balsamea* in the Quebec boreal forest (Canada). Can J For Res 33:190–200

Efron B (1979) Bootstrap methods: another look at the jackknife. Ann Stat 7:1–26

Esper J, Niederer R, Bebi P, Frank D (2008) Climate signal age effects: evidence from young and old trees in the Swiss Engadin. For Ecol Manage 255:3783–3789

Fan ZX, Brauning A, Yang B, Cao KF (2009) Tree ring density-based summer temperature reconstruction for the central Hengduan Mountains in southern China. Global Planet Change 65:1–11

Feng S, Hu Q (2005) Regulation of Tibetan Plateau heating on variation of Indian summer monsoon in the last two millennia. Geophys Res Lett 32:L02702, doi:10.1029/2004GL021246

Fritts HC (1976) Tree rings and climate. Academic Press, London

Goldstein GH, Brubaker LB, Hinckley TM (1985) Water relations of white spruce (*Picea glauca* (Moench) Voss) at tree line in north central Alaska. Can J For Res 15: 1080–1087

Gou X, Peng J, Chen F, Yang M, Levia DF, Li J (2008) A dendrochronological analysis of maximum summer half-year temperature variations over the past 700 years on the northeastern Tibetan Plateau. Theor Appl Climatol 93: 195–206

Helle G, Bräuning A, Schleser GH (2009) Climate history of the Tibetan Plateau for the last 1500 years as inferred from stable carbon isotopes in tree rings. Proc Int Conf Study Environ Change Using Isot Tech, Vienna, April 2001. IAEA CN-80-80:301–311

Holmes RL (1983) Computer-assisted quality control in tree-ring data and measurement. Tree-Ring Bull 43:69–78

Holmes JA, Cook ER, Yang B (2007) Climate change over the past 2000 years in Western China. Quat Int 194:91–107

Körner CH (1999) Alpine plant life: functional plant ecology of high mountain ecosystems. Springer, Berlin

Körner CH, Paulsen J (2004) A world-wide study of high altitude treeline temperatures. J Biogeogr 31:713–732

Lau NC, Nath MJ (2000) Impact of ENSO on the variability of the Asian–Australian monsoons as simulated in GCM experiments. J Clim 13:4287–4309

Li Z, Shi CM, Liu Y, Zhang J, Zhang Q, Ma K (2011) Summer mean temperature variation from 1710–2005 inferred from tree-ring data of the Baimang Snow Mountains, northwestern Yunnan, China. Clim Res 47:207–218

Li ZS, Zhang QB, Ma K (2012) Tree-ring reconstruction of summer temperature for 1475–2003 in the central Hengduan Mountains, Northwestern Yunnan, China. Clim Change 110:455–467

Liang EY, Shao XM, Qin NS (2008) Tree-ring based summer temperature reconstruction for the source region of the Yangtze River on the Tibetan Plateau. Global Planet Change 61:313–320

Liang EY, Shao XM, Xu Y (2009) Tree-ring evidence of recent abnormal warming on the southeast Tibetan Plateau. Theor Appl Climatol 98:9–18

Liang EY, Wang YF, Xu Y, Liu BM, Shao X (2010) Growth variation in *Abies georgei* var. *smithii* along altitudinal gradients in the Sygera Mountains, southeastern Tibetan Plateau. Trees 24:363–373

Liu Y, An Z, Linderholm HW, Chen D and others (2009) Annual temperatures during the last 2485 years in the mid-eastern Tibetan Plateau inferred from tree rings. Sci China D Earth Sci 52:348–359

Michaelsen J (1987) Cross-validation in statistical climate forecast models. J Appl Meteorol Climatol 26:1589–1600

Mitchell TD, Jones PD (2005) An improved method of constructing a database of monthly climate observations and associated high-resolution grids. Int J Climatol 25:693–712

Osborn TJ, Briffa KR, Jones PD (1997) Adjusting variance for sample-size in tree-ring chronologies and other regional mean time series. Dendrochronologia 15:89–99

Rodionov SN (2004) A sequential algorithm for testing climate regime shifts. Geophys Res Lett 31:L09204, doi:10.1029/2004GL019448

Rossi S, Deslauriers A, Gricar J, Seo JW and others (2008) Critical temperatures for xylogenesis in conifers of cold climates. Glob Ecol Biogeogr 17:696–707

Shao X, Wang S, Xu Y, Zhu H, Xu X, Xiao Y (2007) A 3500-year master tree-ring dating chronology from the northeastern part of the Qaidam Basin. Quart Sci 27:477–485

Sheppard PR, Tarasov PE, Graumlich LJ, Heussner KU, Wagner M, Osterle H, Thompson LG (2004) Annual precipitation since 515 BC reconstructed from living and fossil juniper growth of northeastern Qinghai Province, China. Clim Dyn 23:869–881

Thompson LG, Yao T, Mosley-Thompson E, Davis ME, Henderson KA, Lin PN (2000) A high-resolution millennial record of the South Asian Monsoon from Himalayan ice cores. Science 289:1916–1920

Torrence C, Compo GP (1998) A practical guide to wavelet analysis. Bull Am Meteorol Soc 79:61–78

Tranquillini W (1979) Physiological ecology of the alpine treeline. Springer, Berlin

Wang X, Zhang QB (2011) Evidence of solar signals in tree rings of Smith fir from Sygera Mountain in southeast Tibet. J Atmos Sol Terr Phys 73:1959–1966

Wang L, Duan J, Chen J, Huang L, Shao X (2010) Temperature reconstruction from tree-ring maximum density of Balfour spruce in eastern Tibet, China. Int J Climatol 30: 972–979

Wigley TML, Briffa KR, Jones PD (1984) On the average value of correlated time series, with applications in dendroclimatology and hydrometeorology. J Clim Appl Meteorol 23:201–213

Wu G, Zhang Y (1998) Tibetan Plateau forcing and the timing of the monsoon onset over south Asia and the South China Sea. Mon Weather Rev 126:913–927

Xu H, Hong YT, Hong B, Zhu YX, Wang Y (2010) Influence of ENSO on multi-annual temperature variations at Hongyuan, NE Qinghai-Tibet Plateau: evidence from $^{13}C$ of spruce tree rings. Int J Climatol 30:120–126

Yadav RR, Singh J (2002) Tree-ring-based spring temperature patterns over the past four centuries in western Himalaya. Quat Res 57:299–305

Yadav RR, Park WK, Singh J, Dubey B (2004) Do the western Himalayas defy global warming? Geophys Res Lett 31: L17201, doi:10.1029/2004GL020201

Yanai M, Li C (1994) Mechanism of heating and the boundary layer over the Tibetan Plateau. Mon Weather Rev 122:305–323

Yang B, Brauning A, Liu JJ, Davis ME, Yajun S (2009) Temperature changes on the Tibetan Plateau during the past 600 years inferred from ice cores and tree rings. Global Planet Change 69:71–78

Yang B, Kang XC, Brauning A, Liu J, Qin C, Liu JJ (2010) A 622-year regional temperature history of southeast Tibet derived from tree rings. Holocene 20:181–190

Yeh TC, Gao YX (1979) Meteorology of the Qinghai-Xizang (Tibet) Plateau. Science Press, Beijing (in Chinese)

Yu GR, Liu YB, Wang XC, Ma KP (2008) Age-dependent tree-ring growth responses to climate in Qilian juniper (*Sabina przewalskii* Kom.). Trees 22:197–204

Zhang XP, Yao TD, Jin HJ (2000) The influence of ENSO event on the modern $\delta^{18}O$ on the Guliya ice core. J Glaciol Geocryol 22:23–28

Zhang QB, Cheng GD, Yao TD, Kang XC, Huang JG (2003) A 2326-year tree-ring record of climate variability on the northeastern Qinghai-Tibetan Plateau. Geophys Res Lett 30:1739

*Editorial responsibility: Nils Chr. Stenseth, Oslo, Norway*

*Submitted: February 9, 2012; Accepted: November 19, 2012*
*Proofs received from author(s): February 6, 2013*